Indian Journal of Chemical Technology
Vol. 30, May 2023, pp. 352-360
DOI: 10.56042/ijct.v30i3.70650

Solar light driven transition metal codoped ZnO (Ag, Ni- codoped ZnO) photocatalyst for environmental remediation

D Sonia* & E K Kirupa Vasam

Department of Chemistry & Research Centre, Nesamony Memorial Christian College Affiliated to Manonmaniam Sundaranar University, Abishekapatti, Tirunelveli, Marthadam 629 165, India.

E-mail: resolin7@gmail.com

Received 18 January 2023; accepted 29 March 2023

Visible light efficient Ag, Ni-codoped ZnO photocatalyst has been synthesised in the nano form by co-precipitation and sonochemical method using $ZnSO_4 \cdot 7H_2O$ as a precursor. The structural, morphological and elemental observations of synthesised photocatalyst have been characterized using X-ray diffraction (XRD), FTIR, UV-DRS, SEM with EDX and HRTEM analysis. Incorporation of metal ions into ZnO lattice caused a red shift in the absorption band thus extending its absorption towards visible region through inhibition of electron hole recombination reaction and through the property of surface plasmon resonance (SPR). However the addition of silver and nickel ions has modified the electronic and optical properties of the photocatalyst thus improving the photocatalytic performance of the sample. The photocatalytic performance of Ag, Ni-codoped ZnO nanoparticles have been tested for degradation of Direct Red 81 dye (DR-81), as pollutant in aqueous solution. Under the optimum conditions (20 ppm dye and 10 mg/L photocatalyst), complete mineralization of dye solution under study was achieved within 40min of time duration. The Ag, Ni-codoped ZnO photocatalyst is thermally stable and efficient for five successive consecutive runs thus retaining its efficiency towards degradation. The overall results thus obtained have suggested that a suitable method for the detoxification of environmental pollutants emerging from industries.

Keywords: Azo dye, Direct Red 81, Photocatalysis, Textile wastewater, Visible light, ZnO

In modern days, the importance of wastewater treatment, management and disposal is gradually increasing. This poses a major challenge to public health scientific interest[1]. The straight ejection of wastewater effluents into environment causes a dangerous problem, since they have complex mixture of chemical substances and dyes that are difficult to biodegrade[2,3]. The biological activity of several aquatic plants and animals underwater as well as a number of other activities, such as photosynthesis, are directly hampered by dyes in wastewater. Many synthetic organic compounds in the form of dye substances are used in the manufacture process of fabric, paper, printing, rubber, food, cosmetics, and plastic industry[4] that leads high toxicity to environment ecosystem[5]. Additionally, dyes often combine with metal ions to form chelating compounds, which are hazardous to fish and other species. Some of these colours exhibit toxic and carcinogenic characteristics, which has an immediate negative impact on people[6].

Hence, it is a vital task to remove such dyes from the industrial effluent previously discharging into various water bodies[7]. The available water treatment technologies such as absorption, coagulation, sedimentation, filtration chemical and membrane approaches are not so much effective to degrade dyes completely from the atmosphere[8,9]. Consequently, there is a requirement of novel approaches for the removal of harmful complex mixture of chemical substances and dyes for mankind[10].In recent years, one of the most suitable way to eliminate textile contaminants are their degradation by photocatalysis. Indeed, dyes absorb in the visible region and degrade in the presence of photons when irradiated with visible light. Due to their widespread use in organic synthesis and its environmental applications, metal oxide nano particles have attracted particular attention in past decades[11,12].

In recent years, one of the most suitable way to eliminate textile contaminants are their degradation by photo catalysis. Photocatalysis is an advanced oxidation process (AOPs) which extremely depends upon the formation of a strong oxidizing agent like hydroxyl radical, which has a tendency to eradicate the contaminants from wastewater[9,13]. Semiconductor

nanomaterial absorbs greater energy than its band gap energy which leads to the excitation of electrons from the valence band to the conduction band, subsequently producing electrons and holes. When a metal oxide nano particles as a photocatalyst is exposed to UV-Vis radiation, electrons are stimulated from the valence band to conduction band and an electron-hole pair is created[13].

Then the valance band holes can react easily with surface-bound H_2O to produce hydroxyl ($OH^{\bullet}$) radicals, whereas, the electron can react with oxygen (O_2) molecules to produce superoxide radical anion of oxygen ($O_2^{-\bullet}$)[14,15]. The decolorization of the dye is caused by these free radicals ($OH^{\bullet}$ and $O_2^{-\bullet}$), which are particularly good oxidizers of organic dyes and can rapidly react with them to degrade them into CO_2 and H_2O[13,16].

Known for its carcinogenic properties and toxicity toward both humans and animals, the toxic sulphonated azo-based dye Direct Red 81 was chosen as the synthetic model dye solution for experimentation which is widely used across numerous industries[17,18]. Additionally, it harms the skin and eyes. The dye is readily soluble in water due to the double azo linkage and sulphonic acid group that are present[19]. Therefore, industrial effluent must eradicate such hazardous dye before it contaminates the nearby freshwater streams.

The nano sized semiconductor materials (TiO_2, SnO_2, ZnO, etc) have recently proven to be useful for the dye degradation process because their band gaps have an ultraviolet (UV) region[20,21]. One of the most promising semiconductor nanomaterials for electronic and optoelectronic properties is ZnO NPs, which has largest excitation binding energy (60 meV), band gap (3.37eV), high chemical stability, harmless nature, low cost, and high photosensitivity[20,22]. ZnO NPs were also employed in a wide range of industries, including photocatalysis, optical devices, and cosmetics like sunscreen[23].

As a result, in this study, hazardous organic dyes were removed from industrial effluents using synthesised semiconductor nanomaterials rather than traditional materials.Researchers have recently focused on developing the co-doping of two metal atoms into semiconductor materials in order to achieve a higher photocatalytic degradation process compared to single element doping into semiconductor material.When impurity atoms from transition metals are co-doped with ZnO, that produce a new energy level, where electrons are controlled in this new level overcoming the high rate of electron-hole recombination[24].

More than a few metals are used in order to improve the effectiveness of ZnO by co-doping as (Al,Fe) - ZnO nanoparticles[25], (Al,Co) - ZnO nanoparticles[26], (Ni,Co) - ZnO nanoparticles[27], (Al,Mn) - ZnO nanoparticles[28], (Ni,V) - ZnO nanoparticles[29], etc. Co-doped ZnO nanoparticles are produced using a variety of techniques, including sol-gel, co-precipitation, hydrothermal, thermal hydrolysis, dc thermal plasma method etc[30]. Chemical co-precipitation is the most effective and affordable technique for producing large quantities of pure and co-doped ZnO nanoparticles[31].

In this work, Ag, Ni- codoped ZnO nanoparticles was synthesised using an integrated approach of both co-precipitation and sonochemical method. The nanoparticles were characterised by various spectral techniques including XRD, SEM, EDX, HR-TEM and UV-Visible spectral analysis. The modified ZnO photocatalysts showed complete degradation of Direct Red 81 dye (DR 81), a dye pollutant under study. Thus this work has provided a novel route to synthesise a modified ZnO photocatalyst for environmental remediation.

Experimental Section

The major chemicals used for the present study include as follows; zinc sulphate heptahydrate ($ZnSO_4 \cdot 7H_2O$) (LOBA Chemie, 99.5%), nickel sulphate heptahydrate ($NiSO_4 \cdot 7H_2O$)(Sisco, 98%), silver nitrate ($AgNO_3$) (Merck) and sodium bicarbonate ($NaHCO_3$) (LOBA Chemie, 99.5%). These chemicals were procured for the fabrication of Ag,Ni- codoped ZnO photocatalyst and are used in pristine form. Double distilled water is used in all the experiments. The experimental studies were conducted on sunny days from 10.00 am to 2.00 pm respectively. Direct Red 81dye (DR-81) was used as the pollutant for the present study. The structural formula of DR-81 shown in Fig. 1.

Preparation of Ag,Ni- codopedZnOnanophotocatalyst

A stoichiometric quantity of zinc sulphate heptahydrate was dissolved in 100 mL double distilled water under continuous stirring. To this suspension an adequate quantity of nickel sulphate heptahydrate and silver nitrate were added. $NaHCO_3$ solution was added drop wise to the above solution and continuous stirring was done for about5h. The

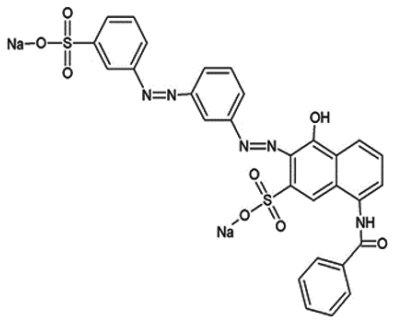

Fig. 1 — Structure of Direct Red-81dye

resultant solution was stirred, and sonicated for an hour. The suspension was centrifuged and washed several times with double distilled water and ethanol, dried at 90°C for 4 h. Finally the Ag, Ni- codoped ZnO nanoparticles was calcinated in a muffle furnace at 450° C for 1 hour and used for further analysis[32].

Characterization techniques

The crystallography information of the photocatalyst was examined using X-ray diffractometer (XRD) using CuKα irradiation (λ = 0.154 nm) operatedwith 40 kV and with 100 mA in the diffraction range (2θ) between 20 to 80°. The average crystalline size i.e. (nm), of the obtained nanoparticles was calculated by Scherrer's equation[32].

$$D=K\,\lambda/\beta\cos\theta \quad ...(1)$$

Where D is the crystallite size, λ is the wavelength of the X-ray used,θ is the diffraction angle, K is the shape factor and βis the full width at half maximum (FWHM) measured in radians.

The surface morphology and shape of Ag, Ni-codoped ZnO nanoparticles were analysed by scanning electron microscope (JEOL, 5800LV) with energy dispersive and X-ray Spectroscopy(JSM-7100F) for analysing the chemical composition of nanoparticles. The morphology and average size of the nanoparticles were analysed by HRTEM (JEOL-2100).

The surface functional entities of Ag, Ni- codoped ZnO nanoparticles were studied using Fourier Transform Infrared Spectroscopy (FT-IR, 8400S Shimadzu, Japan). The optical absorption properties were analysed from UV- Vis diffuse reflectance Spectra (Agilent Cary 5000) using a double beam spectrophotometer within a range of 200-600 nm. The optical band gap of nanoparticles is calculated by Tauc equation Eq. (1)[33].

$$\alpha h\nu = A\,(h\nu - Eg)^n \quad ... (2)$$

where, α is absorption Coefficient, $h\nu$ is photon energy, Eg is band gap, A is constant and n refers to the index which depends on the type of transition. The band gap can be determined from the extrapolation of the straight line to Zero absorbance, i.e. $(\alpha h\nu))^2 = 0$.

Photocatalytic degradation experiments

The photocatalytic activities of synthesised Ag, Ni-codoped ZnO nanoparticles was assessed by evaluating the photocatalytic degradation of an aqueous solution of Direct Red - 81 dye in the presence of visible light at neutral *p*H. Initially 20 ppm of dye solution is taken in a reactor and a small dose of Ag, Ni- codoped ZnO nps (10mg) is added. The suspension was stirred in dark for 30 min to obtain absorption - desorption equilibrium and was placed under direct sunlight with constant stirring. Aliquot of test solution was withdrawn at equal intervals of time, centrifuged and the concentration of sample was analysed by using UV- Visible spectrophotometer. The following equation was used to determine the dye degradation efficiency.

$$\%\ \text{Degradation} = (C_0 - C_t)/C_0 \times 100 \quad ... (3)$$

C_0refers to the initial concentration of the test solution with adsorption-desorption equilibrium and C_t denotes the concentration of the solution after photocatalytic degradation.

Mineralization studies

The degradation of organic material in the contaminant is revealed by an insignificant decrease in the chemical oxygen demand (COD) values. This technique involves the oxidation of the contaminant by potassium dichromate using a strong oxidizing agent. The percentage of mineralization is represented as follows:

$$\%\ \text{mineralization} = (COD_0 - COD_t)/COD_0 \times 100 \quad ...(4)$$

where, COD_0 = initial COD of pollutant dye,

COD_t= COD of dye after irradiation at time‘t’.

Results and Discussion

X-ray diffraction analysis

Figures 2(a) and 2(b) shows the XRD pattern of pure and Ag,Ni- codopedZnOnanoparticles in the 2θ range of 20-80^0. The XRD diffraction peaks at31.67^0, 34.41^0, 35.97^0, 47.52^0, 56.54^0, 62.58^0, 66.3^0, 67.87^0, 68.98^{0}and 76.20^{0}are characteristic to the wurtzite hexagonal phase of ZnO and the peaks corresponds to (100), (002), (101), (102), (110), (103), (200) (112), (201) and (202) planes of ZnO respectively which are

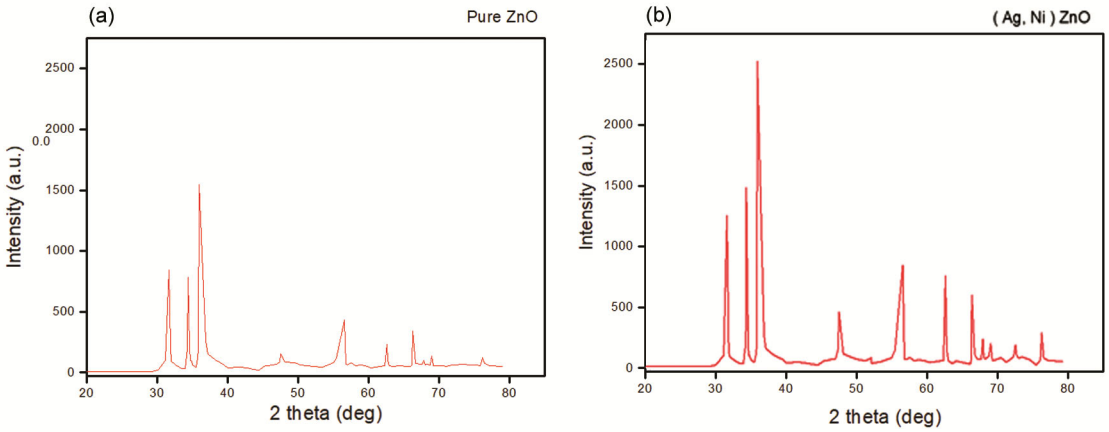

Fig. 2 — X-ray diffraction (XRD) pattern of (a) pureZnO (b) Ag,Ni- codoped ZnO

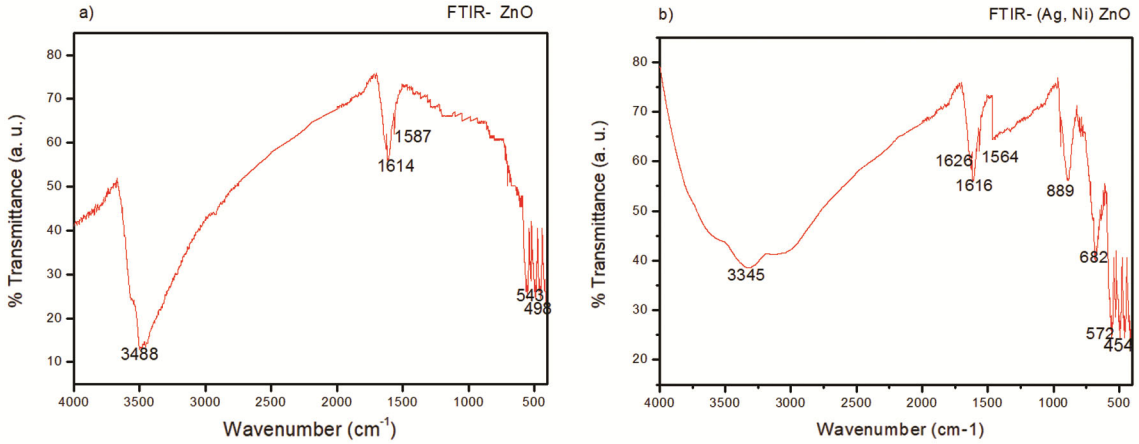

Fig. 3 — FT-IR spectra of (a) pureZnO (b) Ag,Ni- codoped ZnO

in good agreement with the JCPDS file (JCPDS card no 036 - 1451)[34]. The presence of sharp peak at 2θ angle of 35.97^0 for the plane 101 reflects the crystalline nature of the sample. Similar diffraction pattern is reported by Srithar *et al*.[35].

Doping ZnO framework with Ag and Ni ions increased the peak intensities to a greater extent than pure ZnO nanoparticles. This is due to the difference in ionic radii of Ni^{2+} (0.55 A°), Ag^{+} (0.115 A°) and Zn^{2+} (0.60 A°) ions[36]. However, the diffraction peaks characteristic to Ag and Ni ions is missing since the concentration of dopants incorporated into the ZnO crystalline lattice is very low. The crystallite size of the nanoparticles was estimated by using the Debye-Scherrer formula. The average crystallite size of the pristine and Ag, Ni- codoped ZnO nanoparticles are in the range of 23.53 nm and 17.2 nm respectively. The size reduction is attributed to the improved crystallinity of the particles.

FT-IR analysis

The functional group, purity and the molecular structure of the prepared sample is well established from FT-IR spectra performed in the range of 4000-400$cm^{-1}$and the presence of functional groups in ZnO NPs and Ag, Ni- codoped ZnO are shown in Figs. 3(a) and 3(b) respectively.

The band that appears at around 3400 cm^{-1} is an indication of O-H stretching vibration, while the band that appears at around 1615 cm^{-1} is a sign of H-O-H bending vibration. These bands result from a trace amount of H_2O on the ZnO nanocrystalline surface, which may be the result of moisture. These bands are caused by a trace amount of H_2O, which may be moisture, on the ZnO nanocrystalline surface[37].

Several absorption peaks are observed between 400 to 600 cm^{-1} in both the spectra that corresponds to the stretching vibrations of Zn-O bond[38] whereas the absorption peaks in Fig. 3(b) at 454, 889, 1626 and 3345 cm^{-1} are characteristic to the formation of Ni doped in ZnO nanoparticles[39]. The vibrational mode at 889 cm^{-1} is also associated with the incorporation of Ni^{2+} ions occupying at Zn^{2+} sites[40]. Amor Sayari *et al.* also reported same results in an analysis of ZnO NPs doped with Ni and Al[41]. Inclusion of Ag^{2+} ions in ZnO lattice was confirmed by the emergence of new bands at 682 cm^{-1}, which does not exist on the pure form of ZnO NPs[41]. The observed FT-IR spectra of Ag, Ni- codoped ZnONPs clearly indicated that there is no additional chemical bonding presence between the Ag-Ni co-dopants. The result obtained is in consistent with the XRD results reported in Figure 2.

UV-Vis DRS studies

Figure 4 illustrated the UV-Vis absorption spectra of Ag,Ni- codoped ZnO nanoparticles. The optical absorption spectra of synthesized Ag, Ni- codoped ZnO nanoparticles were examined by UV-Vis DRS at room temperature in the range of 200 to 700nm. The optical energy gap of the nanoparticles was obtained from drawing the graph of $(\alpha hv)^2$ versus energy (hv) according to Tauc's equation[42] and the plot is shown in Fig. 5.

ZnO has been considered to be direct band gap oxide and it has a strong absorption maximum towards UV radiation. It has a band gap energy value of the 3.36 eV[41] which has been reported earlier. However its response towards visible region is achieved by incorporation of silver and nickel ions into ZnO lattice. The Ag, Ni- codoped ZnONPs showed an absorption peak edge to 365 nm. This is due to the incorporation of Ag and Ni ions into lattice by filling excessive energy levels on the edge of the conduction level.

Doping ZnO with Ni^{2+} and Ag^{2+} caused the mixing the 3d levels of these ions with 2p orbitals of O^{2-} ions that created a new energy level below the conduction band of ZnO and thus band gap of Ag, Ni- codoped ZnO has decreased to a value of 2.86 eV (Fig. 5). The energy band and the absorption edge of co-doped ZnO photocatalyst showed a red shift due to the exchange interactions caused by sp-d interactions between the electrons of band and localised d orbitalsthus showed a very high visible-light harvesting ability. This could be achieved only after the incorporation of noble metals into the lattice sites of ZnO semiconductor[43,44].

SEM with EDX analysis

The elemental composition and the surface morphology were studied by SEM with EDX analysis and shown in the Figure 6. The Fig. 6(c) and 6(d) showed that the synthesised Ag, Ni-codoped ZnO nanoparticles are agglomerated and appearedas a non-homogeneous spherical particles. EDX spectrum (Fig. 7) shows the atomic % of Ag-Ni ZnO chemical composition in the synthesized Ag,Ni- codoped ZnO nanoparticles, which confirmed the presence of Zn, O, Ag and Ni in the ZnO lattice. Doping of Ag-Ni with ZnO with has not affected the morphological appearance due to very small concentration of dopants incorporated in the lattice of ZnO.

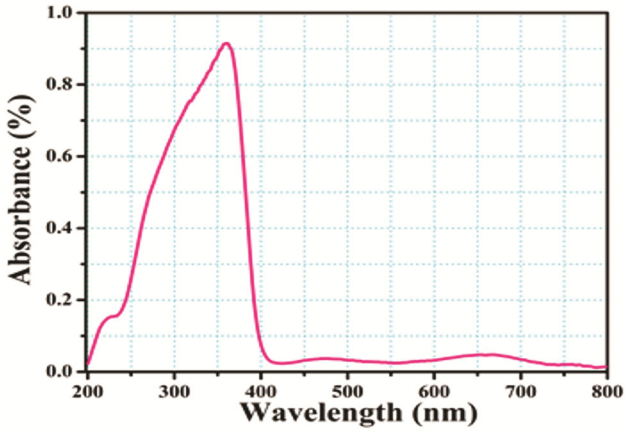

Fig. 4 — UV-Vis absorption spectra of Ag,Ni- codoped ZnO

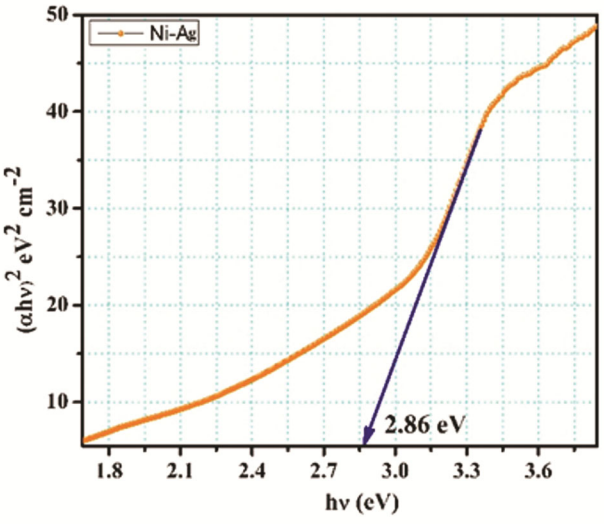

Fig. 5 — Optical band gap spectra of Ag,Ni- codoped ZnO

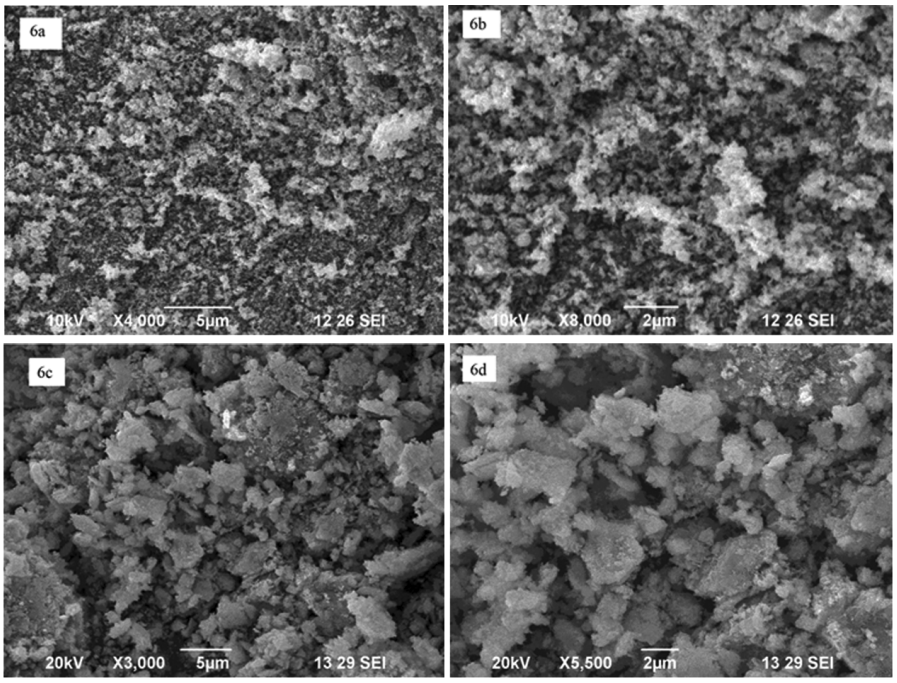

Fig. 6 — SEM images of (a), (b) pureZnO (c), (d) Ag,Ni- codoped ZnO

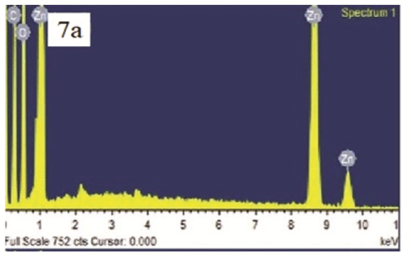

Elements	Weight percentage	Atomic percentage
Zinc	67.4	35.18
Oxygen	32.6	64.82

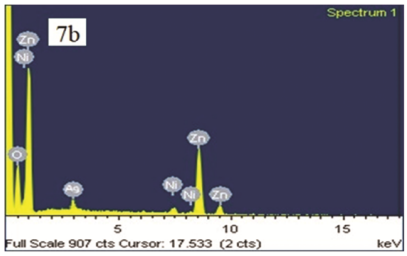

Elements	Weight percentage	Atomic percentage
Zinc	64.63	33.58
Oxygen	28.47	60.44
Silver	2.77	1.60
Nickel	4.13	4.38

Fig. 7 — EDX pattern of (a) pure ZnO and (b) Ag,Ni- codoped ZnO

TEM Analysis

The morphology and particle size of Ag, Ni- codoped ZnO is further characterized by HR-TEM which showed the direct information about the distribution of metal oxide on the surface. Fig. 8(a), 8(b) and 8(c) shows the high-resolution TEM images of Ag, Ni- codoped ZnO photocatalyst. Fig. 8, suggests that, the particles of Ag,Ni- codoped ZnO photocatalyst were spherical in shape and their size were distributed from 10-30 nm. The particle size distribution histogram obtained by Guassian fitting method is shown in Fig.6c and confirms the average particle size of Ag, Ni- codoped ZnO as 17.35 nm, which is in good agreement with the XRD results.

Photocatalytic degradation studies

The photocatalytic decomposition reaction of DR-81, dye was carried out using Ag, Ni- codoped ZnO nanoparticles as photocatalyst under direct sunlight. Figure 9 shows a snapshot of DR-81 dye

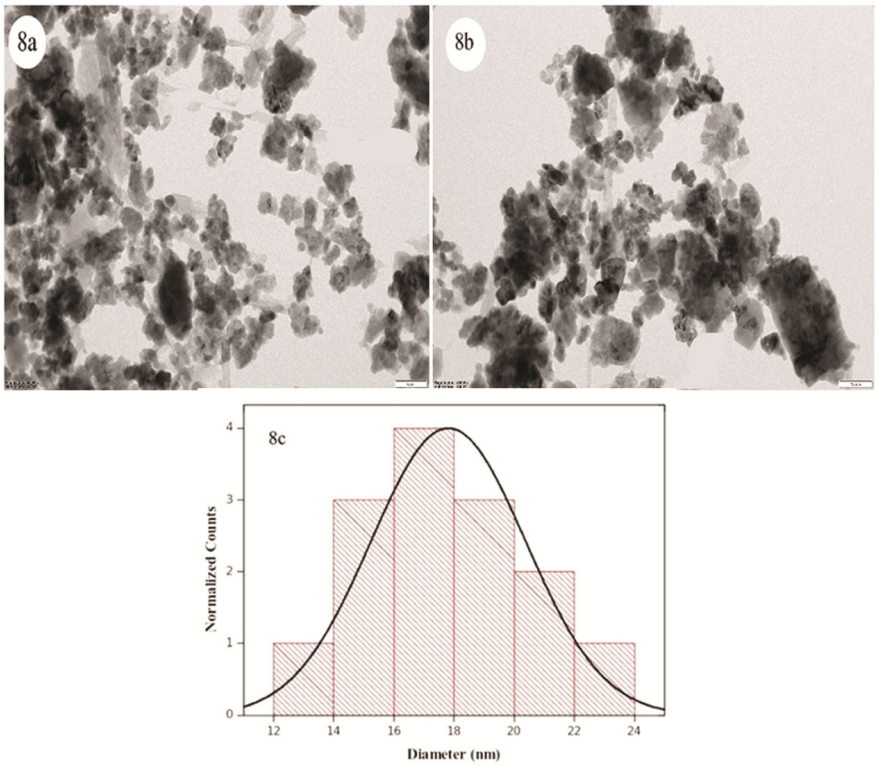

Fig. 8 — HR-TEM images of (a), (b) Ag,Ni- codopedZnO nanoparticles, (c) particle size distribution of Ag,Ni- codoped ZnO

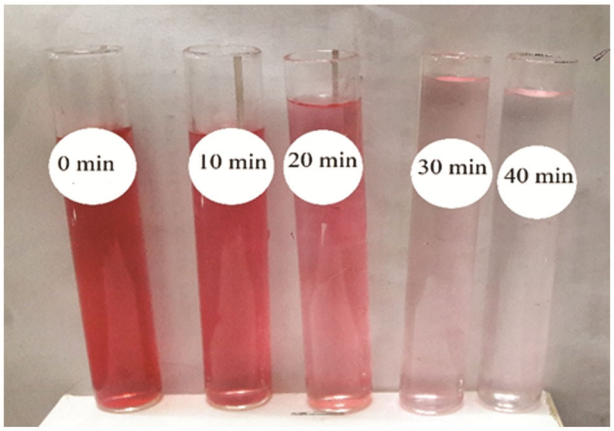

Fig. 9 — Visual representation of photocatalytic degradation experiment

colour removal efficiency using Ag, Ni- codoped ZnO nanoparticles with varying irradiation time intervals (0-40 min). Within forty minutes of irradiation, the colour of the test solution changed from red to a clear colourless liquid, indicating 100 % degradation in the presence of sunlight.

UV-Vis spectral analysis

The degradation of DR-81 dye with Ag, Ni- codoped ZnO photocatalyst was analysed at regular intervals of

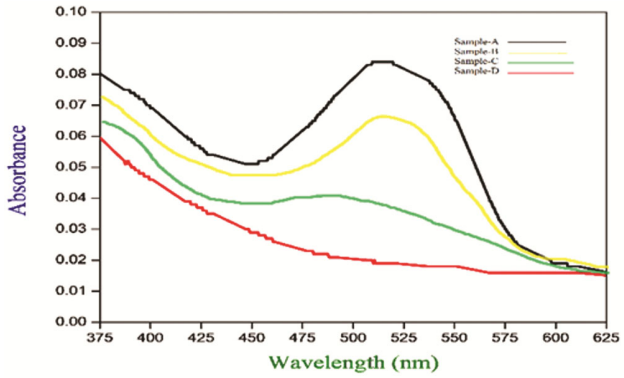

Fig. 10 — UV-Visible absorption spectrum for degradation at various time intervals

irradiation time using UV-Vis absorption spectra and is shown in Fig. 10. DR-81 showed an absorption maxima at λ_{max} =507 nm. However the intensity of absorption maxima of the dye solution under study gradually decreased and finally disappeared completely after 40 min of irradiation using sunlight in the presence of Ag, Ni- codoped ZnO photocatalyst. This ensures the complete degradation of the dye solution.

Photocatalytic mineralization of Direct Red-81

COD analysis was carried out under optimum condition to confirm the mineralization of the DR-81

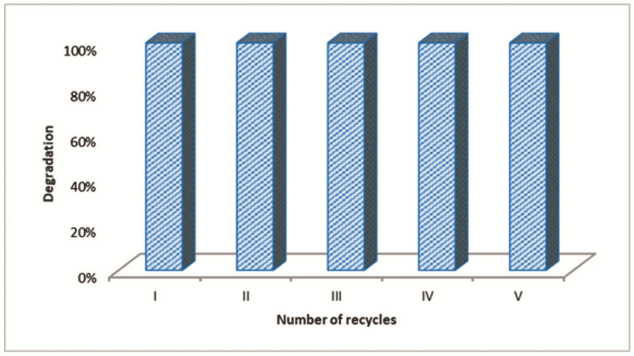

Fig. 11 — Reusability test of Ag,Ni- codoped ZnO

dye. The COD of the dye solution before and after photocatalytic irradiation was estimated to be 14599 and 30 mg/L respectively. These results confirmed the complete mineralisation of dye using the synthesised Ag, Ni- codoped ZnO photocatalyst under optimum conditions showing 99.79% mineralization.

The % mineralization from COD values was calculated as,

$$\% \text{ mineralization} = (COD_0\text{-}COD_t)/COD_0 \times 100$$

Reusability of the catalyst

The cost and stability of the photocatalyst is significantly increased by the reusability of the photocatalyst[45]. Figure 11 represents the reusability of the catalyst. After the degradation experiments were performed the photocatalyst was removed from the dye solution carefully by centrifugation under 3200 rpm. The recovered nanoparticles were washed with double distilled water for several times, dried in an oven to 100°C and further employed for the degradation studies of DR-81. The degrading efficiency is the same for almost five consecutive runs further, as confirmed by UV-visible absorption data. Therefore, it can be concluded that the recycled catalyst can be reused for the photocatalytic degradation of dyes under the influence of sunlight.

Conclusion

A novel photocatalyst Ag, Ni-codoped ZnO, for the degradation of environmental pollutants in aqueous solutions, has been effectively synthesized using an integrated approach of both co-precipitation and sonochemical method with less expensive precursors. The XRD, SEM-EDX and HR-TEM analysis highlight the different optical, morphological and structural characteristics of synthesised Ag, Ni-codoped ZnO photocatalyst than bare ZnO. XRD patterns reveal that the Ag, Ni- codoped ZnO sample has a hexagonal wurtzite structure with an average crystallite size of ~17.2 nm. The particle size distribution histogram has been obtained using Guassian fitting method and confirms the average particle size of Ag, Ni- codoped ZnO as 17.35 nm which is in consistent with XRD analysis. These results are a clear indication of the substitution of Ag and Ni ions into the ZnO lattice. The removal of DR-81was 100 % in the presence of Ag, Ni- codoped ZnO and this enhancement in photocatalytic activity compared to ZnO photocatalyst is due to the increase in the life time of charge carriers. The COD value has decreased to 30 mg/L using sunlight illumination under 40 min. The photocatalyst thus developed show an increased photocatalytic activity, low dosage and is efficiently stable for almost five consecutive runs. Thus the incorporation of silver and nickel ions into ZnO has made an effective technique to enhance the photocatalytic performance of semiconductors in environmental remediation applications.

Acknowledgement

The authors are thankful for Karunya Institute of Technology and Science, Coimbatore, India, Ayya Nadar Janaki Ammal College, Sivakasi, India; and Alagappa University Karaikudi, India for furnishing necessary provision and support for this work.

References

1 Asha S, Bessy T C, Joe S J F, Vijilvani C, Vijaya K C, Bindhu M R, Shanmugam S K, Al Khattaf F S & Hatamleh A A, *Environ Res*, 208 (2022) 112686.
2 Basak S, Pandit P, Samanta K K & Samanta P, *Water Textiles Fashion,* (Woodhead Publishing) (2019) 41.
3 Ashwini R, Sanket J & Joshi, *Open Biotechnol J*, 15 (2021) 97.
4 Amini M & Ashrafi M, *Nanochem Res*, 1 (2016) 79.
5 Xu, Chao Y, Wang, Xing Z, Cheng, Quan X, Xiao, Chang Y & Lu S, *Chem Eng J*, 303 (2016) 555.
6 Baeissa E S, *Front Nanosci Nanotech*, 2 (2016) 1.
7 Hossain A, Sadique R A B M, Raihan M J, Nargis A, Ismail I M I, Habib A & Mahmood A J, *Am J Anal Chem*, 7 (2016) 863.
8 Chollom M N, Rathila S, Pillay V L & Alfa D & *Water S A*, 41 (2015) 398.
9 Zhu J, Zhu Y, Chen Z, Wu S, Fang X & Yao Y, *Int J Environ Res Public Health*, 19 (2022) 1.
10 Isai K A & Shrivastava V S, *J Adv Chem Sci*, 1 (2015) 164.
11 Dodoo A D, Asiedu T, Agyei T B, Nyankson E, Obada D & Mwabora J M, *Mater Today Proc*, 38 (2021) 809.
12 Sivashankar R, Susheeba O K & Velmurugan S, *Res J Chem Environ*, 19 (2015) 48.
13 Isai K A & Shrivastava V S, *S N Appl Sci*, 1 (2019) 1247.
14 Sinar M S I, Mohd L I, Muhd F K & Mastuli M S, *Catalysts*, 10 (2020) 1260.
15 Balcha A, Yadav O P & Dey T, *Environ Sci Pollut Res Int*, 23 (2016) 25485.

16 Lavand A B & Malghe Y S, *J King Saud Univ Sci*, 30 (2018) 65.
17 Sivakumar B, Karthikeyan S & Kannan C, *Dig J Nanomater Bios*, 5 (2010) 657.
18 Heravi1M M, Abasion Z, Morsali A, Ardalan P & Ardalan To, *J Appl Chem*, 9 (2015) 17.
19 Sharma N, Tiwari D P & Singh S K, *Rasayan J Chem*, 7 (2014) 399.
20 Ayaza S, Amin R, Koyal, Samantray, Dasgupta A, Sen S & Tunable, *J Alloys Compd*, 884 (2021) 161113.
21 Giovanni C J, Parrino F, Palmisano G, Scandura G, Citro I, Calogero G, Bartolotta A & Marco G D, *Photochem Photobiol Sci*, 14 (2015) 1685.
22 Hamrounia A, Moussaa N, Paolab A D, Palmisanob L, Houasa A & Parrino F, *J Photochem Photobiol A: Chem*, 309 (2015) 47.
23 Bellarditaa M, El Nazerb H A, Loddoa V, Parrinoa F, Veneziac A M & Palmisano L, *Catal Today*, 284 (2017) 92.
24 El-Bindary A A, Ismail A & Eladl E F, *J Mater Environ Sci*, 10 (2019) 1258.
25 Tariq M, Li Y, Li W X, Yu Z R, Li J M, Hu Y M, Zhu M Y, Jin H M, Liu Y, Li Y B & Skotnicova K, *Adv Manuf*, 7 (2019) 248.
26 Cao P & Bai Y, *Key Eng Mater*, 531 (2013) 299.
27 Fernanda C, Romeiro, Juliane Z, Marinho, Samantha C S, Lemos, Ana P, de Moura, Poliana G, Freire, Luis F, da Silva, Elson Longo, Rodrigo A A, Munoz, Renata C & Lima, *J Solid State Chem*, 230 (2015) 343.
28 Swapna P, Venkatramana R S & Sreenivasulu B, *Res Article*, 10 (2019) 819.
29 Kiruthika R, Radha S, Kirubaveni S & Iyappan G, *IEEE Trans Nanotechnol*, 19 *(*2020) 728.
30 Sankara B, Venkatramana R S, Koteeswara R N & Pramoda K J, *Res J Material Sci*, 1 (2013) 11.
31 Fabbiyola S, John K L, Aruldoss U, Bououdina M, Dakhel A A & Judith V J, *Powder Technol*, 286 (2015) 757.
32 Jeyachitra R, Kalpana S, Senthil T S & Misook K*, Water Sci Technol*, 81 (2020) 1296.
33 Ghomri R, Nasiruzzaman S, Ahmed, Song W, Cai W, Bououdina & Ghers M, *Mater Electron*, 29 (2018) 10677.
34 Reda S M, Khairy M &Mousaa M A, *Arab J Chem*, 13 (2020) 86.
35 Srithar A, Kannan J C & Senthil T S, *J Adv Chem*, 13 (2017) 6273.
36 Naskar A, Lee S & Kim K S, *RSC Adv*, 10 (2020) 1232.
37 Belkhaoui C, Mzabi N, Smaoui H & Daniel P, *Results Phys*, 12 (2019) 1686.
38 Roya E, Khosro H, Afshin M, Reza G, Reza R, Mahdi S, Behzad S, Hiua D, Ali J, Kaan Y & Shivaraju H P*, J Environ Health Sci Eng*, 17 (2019) 479.
39 Loan T T & Long N N, *VNU J Sci: Math Phys*, 30 (2014) 59.
40 Al A S, Nabil A A Y, Al-A'nsi S A, Jumali M H H, Jannah A N & Abd S R, *Sci Reports*, 11 (2021) 11948.
41 Sayari A & Mir L E, *KONA Powder Particle J*, 32 (2015) 154.
42 Prerna, Sandeep A, Asha S, Bikram S, Amit T, Suram S & Rakesh S, *Integ Ferroelectr*, 205 (2020) 1.
43 Chankhanittha T, Naputsawan K, Teeradech S, Jirayus P, Sujittra Y, Khuanjit H & Suwat N, *Colloids Surf A: Physicochem Eng Asp*, 626 (2021) 1.
44 Aliet M Y, Khan M K, Tanveer K A M M, Rahman M M & Kamruzzaman M, *Heliyon*, 6 (2020) 3588.
45 Zeng Q, Liu Y, Liguo S, Hongjun L, Yu W, Xu Y, Li R & Lilin H, *J Colloid Inter Sci*, 582 (2020) 291.